J Solid State Electrochem (2007) 11:451–456
DOI 10.1007/s10008-006-0172-5

ORIGINAL PAPER

Layer-by-layer self-assembled conducting polymer films at elevated pressure investigated by surface plasmon spectroscopy with electrochemistry

N. Zhang · R. Schweiss · W. Knoll

Received: 7 November 2005 / Revised: 4 May 2006 / Accepted: 8 May 2006 / Published online: 8 June 2006

Abstract Polyaniline/sulfonated polyaniline (PANI/SPANI) multilayer films were fabricated using the layer-by-layer (LbL) technique. The electrochemical and optical properties of the film at elevated pressure were investigated by high-pressure surface plasmon spectroscopy combined with electrochemistry. Cyclic voltammograms of the PANI/SPANI films were performed at different hydrostatic pressure. It was found that the charge transfer currents decrease with elevated pressure. This indicates that the film becomes more compact with increasing hydrostatic pressure, which is confirmed by surface plasmon spectra, hinting at a substantial increase in the optical density.

Keywords Surface plasmon resonance · High pressure · Electrochemistry · Layer-by-layer deposition Conducting polymer

N. Zhang · R. Schweiss · W. Knoll
Institute of Materials Research and Engineering,
3 Research Link,
Singapore 117602, Singapore

N. Zhang
Department of Materials Science,
National University of Singapore,
10 Science Drive 4, Lower Kent Ridge Road,
Singapore 117603, Singapore

W. Knoll
Max-Planck Institute for Polymer Research,
Ackermannweg 10,
55128 Mainz, Germany

R. Schweiss (✉)
PTS Heidenau,
Pirnaer Str. 37,
01809 Heidenau, Germany
e-mail: r.schweiss@ptspaper.de

Introduction

Surface plasmon resonance spectroscopy (SPS) makes use of evanescent waves with electromagnetic fields, which decay exponentially in the metal and in the dielectric film. In the latter, the decay length is a few hundred nanometers. This method, therefore, constitutes a highly surface-sensitive tool for probing the optical properties of thin films on noble metal surfaces [1]. It has found many applications in the field of biosensor research and in characterizing surfaces in real time [2]. Recently, a combination of SPS with electrochemical techniques and at high pressure has been developed and some preliminary studies have already been reported [3–5].

The effect of pressure on the optical and electrical properties of polymers used in electronic devices and sensors is very valuable for the further understanding of (opto) electronic phenomena [6]. Previously, high-pressure studies of conducting polymers focused mainly on in situ conductivity and optical spectroscopic studies. Mikat et al. [7–9] studied polypyrrole at high pressure using infrared- and Raman spectroscopy. Likewise, there are a number of papers on the effects of hydrostatic pressure on the DC conductivity of polypyrrole [10–12] and polyaniline [13, 14]. These studies report that hydrostatic pressure increases the conductivity due to a reduction of conjugation defects and also triggers a transition from polarons to bipolarons as the predominant charge carriers. However, little is known about the effect of pressure on the electrochemical properties of conducting polymer films. The layer-by-layer deposition introduced by Decher [15] is a widely used and simple technique for fabricating polymer thin films with nanoscale control of film properties. The adsorption process is driven by electrostatic self-assembly in which polycations and polyanions are alternately deposited on the substrate and has been

reported for a number of conjugated ultrathin polymer films [16–20]. Understanding the properties of these films deposited on an electrode surface is of interest for device applications such as for light-emitting diodes or in biosensors.

In this study, PANI/SPANI multilayer films were investigated by means of high-pressure surface plasmon spectroscopy coupled to an electrochemical cell.

Materials and methods

Polyaniline (PANI) was made water-soluble according to a procedure developed by Rubner et al. [19]. The emeraldine base of polyaniline (Aldrich, MW 65,000) was dissolved in dimethylacetamide at a concentration of 20 mg/ml. The solution was stirred overnight and thereafter ultrasonicated for approximately 8 more hours. The solution was then passed through a glass filter to remove fine particulates (presumably crystalline polyaniline). The polyaniline dipping solution was prepared by slowly adding one part (by volume) of the filtered polyaniline solution to nine parts of diluted HCl (pH between 2.5 and 2.6). The molarity of the polyaniline solution (emeraldine base) was based on the repeat unit containing two aniline structural units (a benzene ring, an amine unit, a quinoid ring, and an imine unit yielding a repeat unit with M=181). An 5% w/w aqueous solution of sulfonated polyaniline (SPANI) was purchased from Aldrich (M=10,000, S/N ratio ~0.5) and then diluted to 10^{-3} mol/l, based on the repeat unit (molecular weight of M=261). The pH was adjusted to around 2.6 by 0.1 M HCl.

Grating coupler fabrication

Grating couplers for SPS were fabricated by a holographic technique [21] with a slightly modified protocol. A He–Cd laser (KIMMOM, Japan) with a wavelength of 325 nm and an expanded beam was used in the photolithographic process. The angle between the optical axis and a mirror, which is positioned perpendicular to the substrate surface, was fixed to 18.96 °. This arrangement generates an interference pattern that yields a sinusoidal grating with a periodicity of Λ=500 nm in the photoresist layer. The quartz discs, which served as substrates (diameter 1 cm, Sico Technology, Germany), were cleaned by sonication in 2% Hellmanex (Hellma GmbH, Germany) and hydrophobized by vapor–phase reaction with Hexamethyldisilazane (HDMS, Aldrich). A photoresist S1805 (Shipley, Singapore) mixed with thinner P (Shipley, Singapore) was then spin-coated (500 rpm/6 s/3,000 rpm/30 s) onto the quartz discs. Following a softbake step (100 °C for 15 min), the discs were exposed to the He–Cd laser (λ=325 nm, 18 s) using the aforementioned setup and developed for 25 s (CD 30 developper, Shipley, Singapore). After another baking step (120 °C for 20 mins), the holographic grating was transferred into the silica discs by reactive ion etching (Oxford Plasmalab, UK, process gas CHF_3/Ar, 1 min). Photoresist residues were removed by rinsing with acetone. Characterization by AFM and laser diffraction revealed a high-quality grating profile with a grating constant close to Λ=500 nm on the surface of the quartz disc. A 2-nm thick chromium and a 150-nm thick gold film were thermally evaporated (Biemtron, Japan) onto the as-prepared discs with a mask, yielding a gold electrode with a corrugation grating.

Layer-by-layer adsorption

PANI/SPANI multilayers were fabricated according to [16]. The substrate surface was functionalized by immersing the substrate with 3-mercapto-1-propanesulfonic acid (MPSA, sodium salt, 10^{-3} mol/l) solution in ethanol for 1 h. This provides a substrate surface with a uniform negative charge. The MPSA/Au/Cr/glass substrate was immersed in dilute HCl solution for a few seconds before the LbL adsorption. The substrate was then alternately immersed in aqueous solutions of the PANI and SPANI for 15 min until the desired number of layers was achieved. Between each deposition cycle, the substrate was rinsed with dilute HCl (pH 2.7)

Surface plasmon spectroscopy

The grating coupling mode of operation [1, 22, 23] was used for high-pressure surface plasmon resonance spectroscopy. A more detailed description can be found in [3]. Briefly, a p-polarized He–Ne–laser (JDS Uniphase, USA) with a wavelength of Λ=632.8 nm was used to excite surface plasmons. The chopped laser beam is reflected off the as-prepared grating surface, and the angular reflectivity is monitored by means of a photodiode that is read out by a lock-in amplifier phase-coupled to the chopper frequency, yielding a typical surface plasmon angular spectrum. The observed minimum corresponds to the excitation of a surface plasmon mode. For experiments at elevated pressure, a high-pressure steel cell [23] was connected to a syringe pump (Nova Swiss, Switzerland) equipped with a stepper motor and a controller to generate hydrostatic pressure inside the cell.

Electrochemistry

Electrochemical experiments were performed in a three-electrode high-pressure cell using a potentiostat (Princeton Applied Research 263A, EG&G). The reference electrode was Ag-wire quasi-reference electrode. The as-prepared

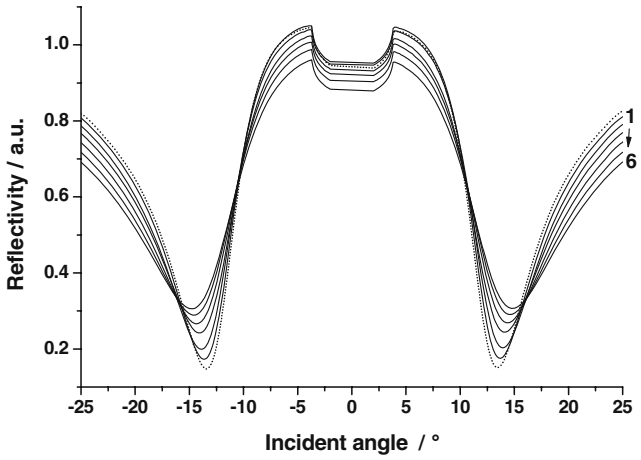

Fig. 1 SPS angular scans of a MPSA-primed gold surface (*dotted line*) and scans taken after each subsequent deposition of six bilayers of PANI/SPANI

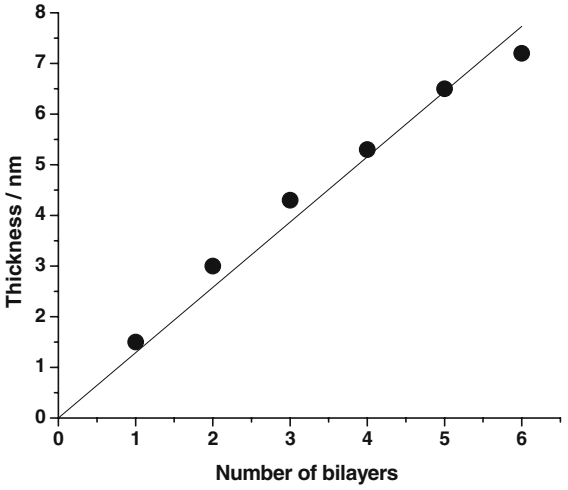

Fig. 2 Thickness of multilayer film vs number of bilayers

Au/Cr/quartz grating coupler was simultaneously used as the working electrode, while a platinum wire served as the counter electrode. All experiments were performed using PBS buffer (0.15 M sodium chloride, 0.02 M phosphate buffer) as an electrolyte.

Results and discussion

PANI/SPANI layer-by-layer assembly

A series of SPS angular scans were taken after each polyelectrolyte bilayer adsorption, as shown in Fig. 1. These scans were recorded in situ after each bilayer deposition in a homemade Teflon flow cell. A shift of the SPS minimum angle to higher angles is observed for each adsorption step. This indicates a continuous deposition of PANI/SPANI layer pairs on the gold surface.

It is inherent in SPS that the thickness and refractive index change of the film cannot be derived separately. From UV–VIS spectroscopy, however, the complex dielectric constant of a PANI/SPANI multilayer film has been previously determined to be $\varepsilon = 2.2 + I \cdot 0.6$ at Λ=633 nm [24]. Figure 2 shows a plot of the thickness as a function of the number of bilayers with the assumed dielectric constant of the film. A linear behavior is observed, which is similar to that reported in the literature [25, 26]. The absolute value is, nonetheless, a little smaller than in these studies. This might be due to the grating profile. In the case of the grating coupler, the surface is not smooth but corrugated, which has some influence on the self-assembly behavior and the structure of the polyelectrolyte film, resulting in a comparatively smaller optical thickness.

Pressure effect on the medium (Reference)

Before we study the PANI/SPANI multilayer film at elevated pressure, the pressure behavior of the pressure medium and the bare gold substrate needs to be quantified to serve as a reference. We recorded SPS angular scans of the bare gold grating in 0.1 mol/l PBS buffer at four different pressures, as shown in Fig. 3.

A shift of the minimum angle to higher values with elevated pressure can be noticed. The shift of the SPS spectrum can be completely fitted by the changing refractive index of the pressure medium (PBS buffer) only. By increasing the pressure, the density of the PBS buffer increases and, consequently, its refractive index also increases. In contrast, the dielectric constants of gold remained unchanged upon fitting. The surface plasmon

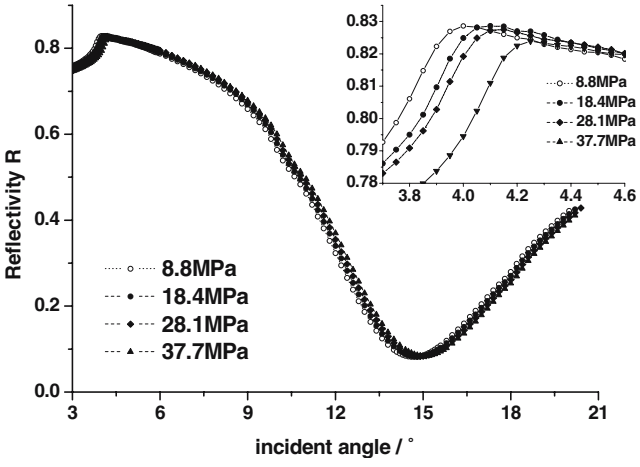

Fig. 3 SPS angular scans of an evaporated gold layer in PBS at different pressures (*inset*: reflectivity near the angle of total internal reflection)

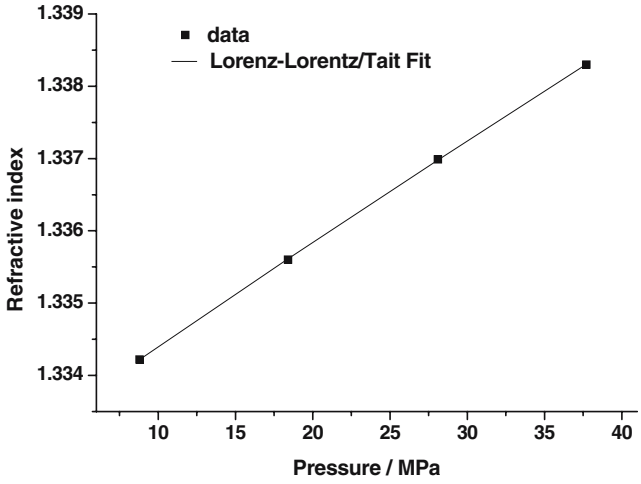

Fig. 4 Refractive index of PBS buffer at different pressures. The *solid line* represents a fit to the data using the Lorenz–Lorentz/Tait equation

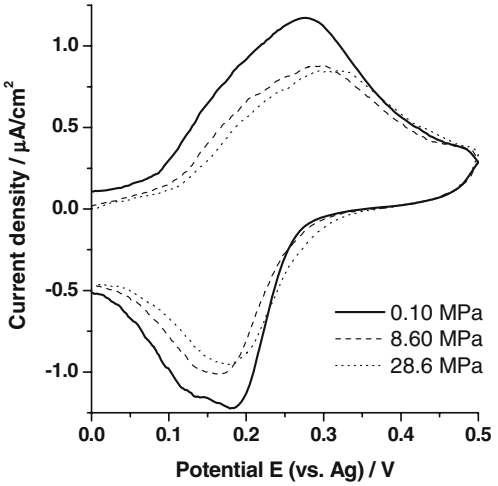

Fig. 5 Cyclic voltammograms of six bilayers of PANI/SPANI in PBS at different pressures (scan rate 20 mV/s)

resonance can be observed across the whole pressure range. Thus, the gold layer is stable and its optical properties can be considered as constant in aqueous environment up to the maximum pressure of 37.7 MPa applied in this study. Figure 4 depicts the refractive index of the PBS buffer as a function of pressure up to 37.7 MPa. With increasing pressure, the compression leads to an increased density of the medium and, thus, an increased refractive index. As shown in Fig. 4, this behavior could well be fitted to the Lorenz–Lorentz-Tait equation [23]

$$R_{LL} = \frac{1}{\rho_0}\left\{1 - \alpha_0 B(T)\cdot ln\left[\frac{B(T)+p}{B(T)+p_0}\right]\right\} \cdot \left(\frac{n^2-1}{n^2+1}\right), \quad (1)$$

where α_0 is the bulk compressibility and ρ_0 the density at standard conditions ($p0$=1.013·10^5 Pa and T_0=25 °C), B(T) the first virial coefficient (Tait parameter) and R_{LL} the Lorenz–Lorentz constant, respectively.

Electroactivity of multilayer films at elevated pressure

Next, the substrate with PANI/SPANI multilayer films was introduced into the high-pressure electrochemical SPS cell. The cyclic voltammograms of the PANI/SPANI film in PBS at different pressure were measured and compared. Figure 5 presents the cyclic voltammograms at a scan rate of 20 mV/s. As reported previously, a broad redox peak is observed, which is the result of an overlap of two redox processes [16, 24]. For the PANI/SPANI multilayer film, the PANI is doped by the negatively charged SPANI, which is the charge carrier in the film. It can be seen that the peak current decreases from 0.1 to 28.6 MPa and that the peaks are shifted to larger potentials. This indicates that the film becomes more compact under elevated pressure, thus impeding the redox reaction. It could also be that elevated pressure leads to a perturbation of the highly ordered anionic–cationic layer structure, which, in turn, could result in a loss of electrochemical activity. To investigate the system further, the sweep rate was varied at constant pressure.

In Fig. 6, the cathodic peak current is plotted as a function of the square root of the sweep rate. It can be fitted by a straight line, indicating a diffusion-limited redox process. The slopes decreased with the applied pressure, thus indicating that the apparent diffusion of the redox centers is slower in the more compact film.

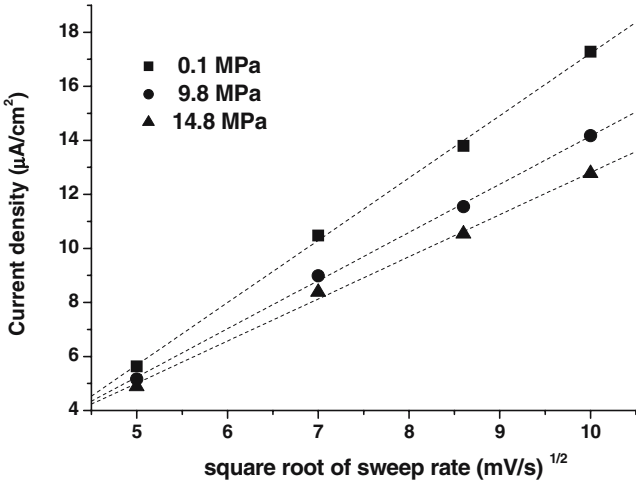

Fig. 6 Cathodic peak current vs square root of the scan rate at different pressures. The *dashed lines* are linear fits to the data

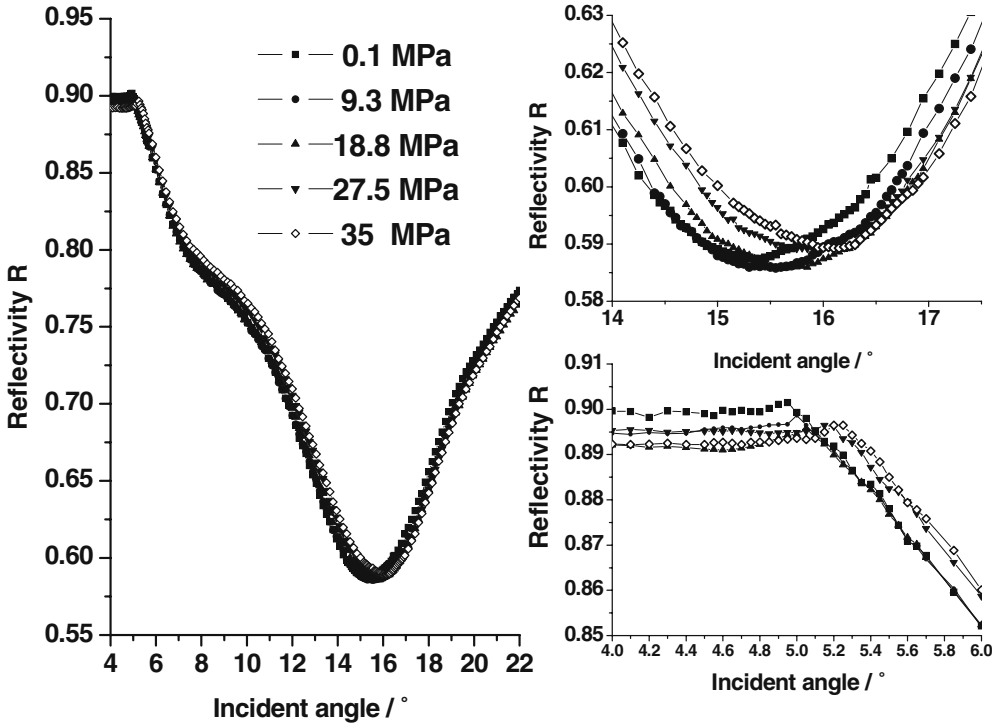

Fig. 7 SPS angular scans of a PANI/SPANI multilayer film (reduced state) in PBS at different pressures. **a** Full scan, **b** near the SPR resonance angle θ_m, **c** near the angle of total internal reflection, θ_c

Optical properties of multilayer films

The optical properties of PANI/SPANI multilayer films at elevated pressure were investigated by SPS. Figure 7 shows the SPS angular scans at different pressures. It can be observed that the resonances shift to higher angles. Resonance shifts including the reference system (bare gold/PBS) are depicted in Table 1.

It is obvious that the angle shifts are larger in the gold/$(PANI/SPANI)_n$/PBS system than in the bare gold/PBS system. The spectra could not be fitted by changing the refractive index of PBS only. In other words, the changes in the multilayer film upon application of hydrostatic pressure also contribute to the resonance shift. As discussed previously, the refractive index of PBS increases with elevated pressure, which makes the whole SPS curve shift to a higher angle. From the investigation of the electroactivity of the PANI/SPANI film, we know that the film becomes more compact under pressure and the film density increases accordingly. As a decrease in the film thickness would result in lower coupling angles, we conclude that the prevailing effect, which accounts for the surface plasmon resonance shifts, is an increase in the refractive index of the polymer films.

However, only a set of parameters (n, d) of the film could be derived from a single-wavelength SPS angular scan. These two parameters are correlated and cannot be separated by these SPS angular scans alone. A simple approximation can be made using the bulk compressibility of polyaniline (0.2 GPa^{-1} [13]) and the thickness of the film at standard conditions (obtained using ε=2.1+i 0.4). According to this assumption, the decrease in thickness

Table 1 Comparison of the critical angle and minimum angle of the bare gold/PBS system with those of the PANI/SPANI multilayer film system

		0.1 MPa	8 MPa	18 MPa	28 MPa	38 MPa
Bare gold	θ_c/°	/	4.00	4.05	4.1	4.2
	θ_m/°	/	14.7	14.8	14.9	15
PANI/SPANI film	θ_c/°	4.95	5.0	5.05	5.1	5.15
	θ_m/°	15.4	15.55	15.7	15.85	16.0

θ_c critical angle, θ_m minimum angle

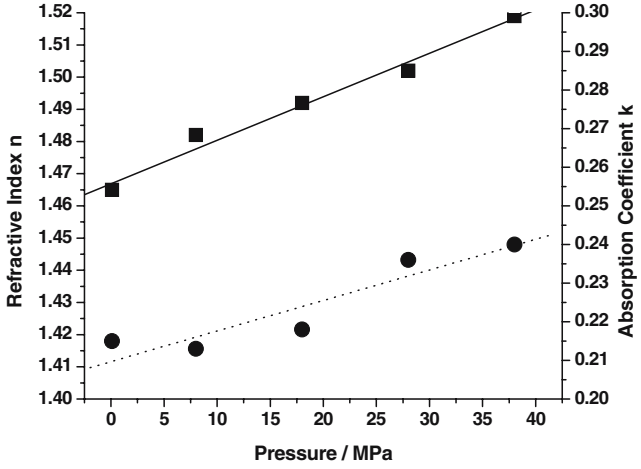

Fig. 8 Calculated refractive index *n* (*squares*, *left axis*) and absorption coefficient *k* (*circles*, *right axis*) of PANI/SPANI films (four bilayers, reduced state) as a function of hydrostatic pressure

should only be 2% at 38 MPa. Taking this into account, the real and imaginary parts of the refractive index both increase with increasing pressure (see Fig. 8).

Conclusion

Multilayer films of PANI/SPANI were prepared by electrostatic self-assembly and studied at elevated pressure. High-pressure electrochemical surface plasmon spectroscopy indicates an increase in the (optical) density together with a decrease in the electro-chemical activity of the multilayer films. Voltammetry experiments provide evidence for a apparent diffusion-limited redox process with lowered diffusion at elevated hydrostatic pressure.

Acknowledgements The authors would like to thank Drs. Akira Baba and Thomas Jakob (both NUS) for their support in the layer-by-layer fabrication process and in High Pressure SPS, respectively. Dr. Jinghua Teng (IMRE) is gratefully acknowledged for providing admission to the laser holographic grating setup.

References

1. Knoll W (1998) Annu Rev Phys Chem 49:569
2. Davies J, Faulkner I (1996) In: Davies J (ed) Surface plasmon resonance—theory and considerations. Surface analytical techniques for probing biomaterial processes. CRC, Boca Raton, Florida
3. Jakob T, Knoll W (2003) J Electroanal Chem 543:51
4. Jakob T, Kleideiter G, Knoll W (2004) Int J Polym Anal Charact 9:153
5. Baba A, Kleideiter G, Jakob T, Knoll W (2004) Macromol Chem Phys 205:2267
6. Drickamer HG (1992) High pressure chemistry, biochemistry and materials science. In: Winter R, Jonas J (eds) NATO ASI Series, p 67
7. Mikat J, Orgzall I, Hochheimer HD (2001) Synth Met 116:167
8. Mikat J (2001) Synth Met 119:649
9. Mikat J, Orgzall I, Hochheimer HD (2002) Phys Rev B 65:174202
10. Lundin A, Lundberg B, Sauerer W, Nandery P, Naegele D (1990) Synth Met 39:233
11. Maddison DS, Tansley TS (1992) J Appl Phys 71:1831
12. Orgzall I, Lorenz B, Dunsch L, Bartl A, Ting S, Hor PH, Hochheimer HD (1996) Synth Met 81:59
13. Lundberg B, Salaneck WR, Lundstroem I (1987) Synth Met 21:143
14. Bao XB, Liu CX, Pahol, PK, Pinto NJ (1999) Synth Met 106:107
15. Decher G (1997) Science 277:1232
16. Tian S, Baba A, Liu J, Wang ZH, Knoll W, Park MK, Advincula R (2003) Adv Funct Mater 13:473
17. Ferreira M, Cheung JH, Rubner MF (1994) Thin Solid Films 244:806
18. Ferreira M, Rubner MF (1995) Macromolecules 28:7107
19. Cheung JH, Stockton WB, Rubner MF (1997) Macromolecules 30:2712
20. Schlenoff JB, Laurent D, Ly H, Stepp J (1998) Adv Mater 10:347
21. Mai X, Moshrefzadeh R, Gibson UJ, Stegeman GI, Seaton CT (1985) Appl Opt 24:3155
22. Kambhampati DK, Jakob TAM, Robertson JW, Cai M, Pemberton JE, Knoll W (2001) Langmuir 17:1169
23. Kleideiter G, Sekkat Z, Kreiter M, Lechner M, Knoll W (2000) J Mol Struct 521:167
24. Baba A, Park M, Advincula RC, Knoll W (2002) Langmuir 18:4648
25. Advincula R, Frank, CW, Roitman D, Sheats J, Moon R, Knoll W (1998) Mol Cryst Liq Cryst 316:103
26. Mark H, Rubinson JF (1999) Conducting polymer films as electrodes. In: Wieckowski A (ed) Interfacial electrochemistry; principles and applications. Marcel Dekker, New York, p 839